ELSEVIER

Journal of Organometallic Chemistry 649 (2002) 100–107

Journal of Organometallic Chemistry

www.elsevier.com/locate/jorganchem

Rydberg spectra of bis(η⁶-benzene)chromium derivatives Gas-phase photoabsorption study of bis(η⁶-1,2,4-trimethylbenzene)chromium and bis(η⁶-1,2,4,5-tetramethylbenzene)chromium

Sergey Yu. Ketkov [a,*], Georgy K. Fukin [a], Lev N. Zakharov [a], Jennifer C. Green [b,*], Gerald Clancy [b]

[a] *G.A. Razuvaev Institute of Organometallic Chemistry of the Russian Academy of Sciences, Nizhniy Novgorod 603600, Russian Federation*
[b] *Inorganic Chemistry Laboratory, University of Oxford, South Parks Road, Oxford OX1 3QR, UK*

Received 8 November 2001; received in revised form 14 December 2001; accepted 14 December 2001

Abstract

The gas-phase electronic absorption spectra of $(\eta^6\text{-}1,2,4\text{-}C_6H_3Me_3)_2Cr$ (**1**) and $(\eta^6\text{-}1,2,4,5\text{-}C_6H_2Me_4)_2Cr$ (**2**) have been measured for the first time and compared with those recorded in *n*-pentane solution. The gas-phase spectra of both compounds show transitions from the non-bonding chromium $3d_{z^2}$ orbital to molecular Rydberg s, p and d levels. The first ionisation potentials have been determined from the Rydberg frequencies as 4.994 ± 0.009 and 4.862 ± 0.009 eV for **1** and **2**, respectively. Detailed assignments of Rydberg bands have been made on the basis of analysis of the quantum defects and term values. The Rydberg structures agree with the C_1, C_s or C_2 conformation for **1** and the D_{2d} geometry for **2** in the gas phase. In crystal, however, the molecule of **2** appears to adopt an eclipsed conformation close to D_{2h} as indicated by the X-ray diffraction. The influence of ring methylation on the Rydberg term values has been analysed for the first time.

Keywords: Rydberg spectroscopy; Electronic absorption spectra; Bisarene complexes; Chromium; Methyl substituents

1. Introduction

Bisarene complexes of chromium represent the first class of organometallic compounds showing well-resolved Rydberg transitions in the photoabsorption spectra [1–5]. Narrow Rydberg absorption bands arise from the excitations originating at the highest occupied level which represents the strongly non-bonding metal $3d_{z^2}$ orbital. In the gas-phase spectrum of bis(η⁶-benzene)chromium two Rydberg p series have been found [2,3]. The frequencies of the higher series members obey the well-known Rydberg formula

$$\nu_n = I - R/(n-\delta)^2 = I - R/(n^*)^2 = I - T_n,$$

where I is the ionisation threshold corresponding to detachment of the $3d_{z^2}$ electron, R is the Rydberg constant (109 737 cm^{-1}), n is the principal quantum number, δ is the quantum defect, n^* is the effective principal quantum number and T_n is the term value of a Rydberg transition equal to the binding energy of a Rydberg electron. The first ionisation potential of a sandwich compound can be calculated with high accuracy on the basis of these frequencies [1–5].

In contrast to the solution-phase spectra of chromium bisarene derivatives, the spectra measured in the gas phase appeared to be very sensitive to the presence of substituents in the benzene rings. The gas-phase photoabsorption spectroscopy can give, therefore, new important information concerning substituent influence on the molecular and electronic structures of $(\eta^6\text{-arene})_2Cr$. In our earlier works [2–4], it has been shown that methylation of benzene rings causes changes in the Rydberg structure because of the molecular symmetry reduction. When one goes from bis(η⁶-benzene)chromium to the complexes of toluene, *o*-xylene and *m*-xylene, the lowest $3d_{z^2} \rightarrow Rnp_{x,y}$ transitions split into two components and the $3d_{z^2} \rightarrow Rns$,

* Corresponding authors. Fax: +1-1865-272690.
E-mail address: jennifer.green@chem.ox.ac.uk (J.C. Green).

0022-328X/02/$ - see front matter
PII: S0022-328X(02)01128-2

Rnd bands appear in the absorption spectra. For (η^6-1,3,5-$C_6H_3Me_3)_2Cr$ the $Rnp_{x,y}$ levels are degenerated and the $3d_{z^2} \rightarrow Rns$ transitions become symmetry forbidden [4]. The R4p bands in the spectrum of the mesitylene derivative are weak while the $R5p_{x,y}$ peak is broadened and shifted as a result of the Rydberg-valence mixing [4]. It was impossible, therefore, to study the influence of methyl groups on the Rydberg parameters using the (η^6-1,3,5-$C_6H_3Me_3)_2Cr$ spectrum. We decided to measure the gas-phase electronic absorption spectrum of (η^6-1,2,4-$C_6H_3Me_3)_2Cr$ (**1**) in order to reveal the trends caused by methylation of the rings. It was necessary to study also the changes in the Rydberg structure resulting from the further increase in the number of methyl substituents. So the spectrum of (η^6-1,2,4,5-$C_6H_2Me_4)_2Cr$ (**2**) has been investigated for the first time in this work.

2. Experimental

2.1. Syntheses

All operations, unless otherwise stated, were performed under dry nitrogen or in vacuo. Complexes **1** and **2** were synthesised by co-condensation of chromium atoms and arene vapours at 77 K [6] using the apparatus described elsewhere [7]. After warming the mixture of compound **1** and 1,2,4-trimethylbenzene to room temperature (r.t.), its dissolving in light petroleum, filtration, and removal of organics, complex **1** was isolated by vacuum sublimation. In the synthesis of **2**, toluene was used to dissolve the reaction mixture. To remove traces of durene, the oxidation–reduction cycle was employed. The neutral complex was oxidized by air in the presence of water to give the $\mathbf{2}^+$ cation. The organic impurities were extracted twice by Et_2O and then NaOH and aluminium powder were added to the aqueous solution containing $\mathbf{2}^+$ for its reduction. The neutral compound was dissolved in toluene and sublimed in vacuo after removing the solvent. The purity of bisarene complexes was checked by the element analysis and ^{1}H-, ^{13}C-NMR spectroscopy.

2.2. Photoabsorption measurements

The gas-phase electronic absorption spectra were recorded with a Specord UV–vis (Carl Zeiss, Jena) spectrometer. The best spectroscopic resolution was 30 cm^{-1}. Errors in determination of Rydberg frequencies arose from the bands' broadening and overlapping of neighbouring absorption peaks, typical values being 30–40 cm^{-1} for sharp maxima and 80–150 cm^{-1} for broad bands and shoulders. The gas-phase spectra of **1** and **2** were measured using an evacuated quartz cell heated to 120–160 °C. For comparison, the spectra of the complexes in *n*-pentane solution have been recorded in a vacuum cell with the same instrument at r.t. Rydberg peaks disappeared on going from the gas to the condensed phase in accordance with theory [8]. To find the parameters of overlapping Rydberg bands in the $n = 6$–8 region, Gaussian-fit analysis has been carried out. The experimental spectral lines were decomposed into a sum of symmetric and asymmetric Gaussian components using a home-made computer program which defined the positions, intensities and widths of the peaks by the least-squares method.

2.3. X-ray diffraction of (η^6-1,2,4,5-$C_6H_2Me_4)_2Cr$

To compare the molecular symmetry of gas-phase complex **2** resulted from the analysis of Rydberg transitions with that of the solid-state compound, the crystal structure of **2** has been determined by the X-ray diffraction method. Crystal data for **2**: $C_{20}H_{28}Cr$, $M = 320.42$, monoclinic, $a = 7.044(7)$ Å, $b = 10.417(10)$ Å, $c = 11.042(10)$ Å, $\beta = 100.58(8)°$, $V = 796.4(13)$ Å^3, $T = 293$ K, space group $P2_1/n$ (no. 14), $Z = 2$, $\mu(Mo–K_\alpha) = 0.710$ mm^{-1}, 3456 reflections measured on a Siemens R3 diffractometer, 3208 unique ($R_{int} = 0.023$) which were used in all calculations. The structure was solved by direct methods and refined with anisotropic thermal parameters for the non-H atoms and isotropic for the H atoms. The positions of the H atoms were located on the difference Fourier map. The final *R*-factors were $R = 0.031$, $wR(F^2) = 0.0792$ (all data). The largest difference peak and hole were 0.554 and -0.832 e Å^{-3}. All calculations were performed by the SHELXTL package [9].

3. Results and discussion

3.1. Interpretation of Rydberg structures

The gas-phase electronic absorption spectra of **1** and **2** show well-defined Rydberg structures which can be revealed by comparison with the solution spectra (Fig. 1). In the condensed phase Rydberg transitions of polyatomic molecules are, as a rule, broadened beyond detection because of scattering of a Rydberg electron in the media of low electron mobility and because of intermolecular interactions [8]. Rydberg features disappear, therefore, when one goes from the gas-phase absorption spectra to the spectra of the compounds dissolved in organic solvents. This is clearly seen in Fig. 1. The spectra of **1** and **2** in *n*-pentane show only one broad intense peak A while the spectra of gases reveal many comparatively narrow Rydberg bands besides. Note that spectra of **1** and **2** in the gas-phase are different in contrast to those in solution which are very similar.

The short-wavelength peaks in each gas-phase spectrum form a series converging at the ionisation threshold. The frequencies of the series members are described very well by the Rydberg formula (Table 1).

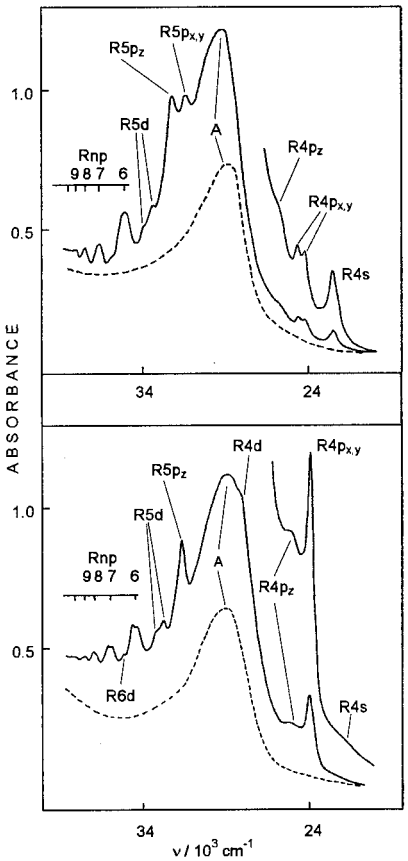

Fig. 1. The electronic absorption spectra of **1** (top) and **2** (bottom) in the gas phase (full line) and in *n*-pentane solution (dashed line).

Table 1
Observed $\nu_{obs.}$ and calculated $\nu_{calc.}$ frequencies (cm^{-1}) of the Rnp ($n = 6$–10) series members in the spectra of **1** and **2**

n	**1**		**2**	
	$\nu_{obs.}$	$\nu_{calc.}$	$\nu_{obs.}$	$\nu_{calc.}$
6	35 400	35 410	34 440[a]	34 440
7	36 970	36 950	35 960[a]	35 950
8	37 870	37 870	36 830	36 830
9	38 450	38 450	37 390	37 400
10	38 840	38 840	37 800	37 790
I	40 280		39 210	
δ	1.25		1.20	
s	12		13	
r	0.99997		0.99996	

For each set of frequencies, the ionisation threshold *I* (cm^{-1}), quantum defect δ, standard deviation *s* (cm^{-1}) and correlation coefficient *r* resulted from the non-linear regression analysis are given.

[a] Averaged values $\nu = (\nu(p_{x,y}) + \nu(p_z))/2$, where $\nu(p_{x,y})$ and $\nu(p_z)$ are the observed frequencies of the $Rnp_{x,y}$ and Rnp_z transitions, respectively.

The non-linear regression analysis gives the standard deviations *s* smaller than 15 cm^{-1} and correlation coefficients *r* higher than 0.9999. The ionisation limit of the Rydberg series equals 40 280 (4.994) and 39 210 cm^{-1} (4.862 eV) for **1** and **2**, respectively. Varying the peak frequencies within the experimental error, and using the procedure of non-linear regression analysis one can obtain the threshold values differing by 50–70 cm^{-1} (0.006–0.009 eV) from those given above. These values correspond to the first ionisation potentials (IP) of **1** and **2** which have not, to our knowledge, been determined before. IP of **1** and **2** can be taken, therefore, as 4.994 ± 0.009 and 4.862 ± 0.009 eV, respectively, on the basis of the data obtained in this work. IP of **1** is very close to that of (η^6-1,3,5-$C_6H_3Me_3$)$_2$Cr (5.004 eV [4]). On the basis of IP the term value *T* and effective principal quantum number *n** can be calculated for each Rydberg feature observed in the spectra of **1** and **2**. These parameters are especially useful when analysing the lower-lying Rydberg transitions in bisarene complexes [1–5]. They are given in Table 2 for the excitations characterised by $n = 4$–7 together with the transition frequencies.

The Rydberg series in the absorption spectra of **1** and **2** arise from the transitions originating at the $3d_{z^2}$ metal-localised molecular orbital (MO) since the first IP of bis(η^6-arene)chromium corresponds to detachment of an electron from this level [10]. The quantum defects (Table 1) are typical for Rydberg p transitions in (η^6-arene)$_2$Cr [1–5]. For the most bisarene complexes studied earlier [1–4], two Rydberg series terminating at the $p_{x,y}$ and p_z levels can be revealed.

Each of the R6p and R7p bands in the spectrum of **2** is split into two peaks (Fig. 1). The Gaussian-fit analysis shows that the peak intensities are close (Fig. 2) so the arithmetic means of their frequencies were used when considering the Rydberg series (Table 1). On the contrary, for complex **1** the two components of the R6p and R7p transitions overlap strongly giving one maximum in each case (Fig. 1). The presence of more than one Rydberg p series in the spectrum of **1** is indicated by the broadening of the R6p band in comparison with the higher series members. Full-width at half-height is 760, 480, and 360 cm^{-1} for the R6p, R7p, and R8p band, respectively. The frequency of each Rydberg p component can be found from the Gaussian-fit analysis (Fig. 2). Thus, Table 1 and Table 2 present different data for the R6p and R7p bands. The former gives the averaged frequencies corresponding to the band maxima for **1** and the arithmetic mean of the two component positions for **2** which is necessary to determine the IP and the averaged quantum defect of the p series. The latter presents the frequency, term value and effective principal quantum number of each p component.

By analogy with other methylated bisarene complexes [4], we should assign the long-wavelength and

Table 2
Frequencies ν (cm^{-1}), term values T (cm^{-1}) and effective principal quantum numbers n^* for transitions of the $3d_{z^2}$ electron to the Rydberg MOs ($n = 4$–7) of **1** and **2**

Rydberg MO	**1**			**2**		
	ν	T	n^*	ν	T	n^*
4s	22 300	17 980	2.47	22 200[a]	17 010	2.54
$4p_{x,y}$	24 010	16 270	2.60	23 980	15 230	2.68
$4p_{x,y}$	24 480	15 800	2.64	–	–	–
$4p_z$	25 400[a]	14 880	2.72	25 110[a]	14 100	2.79
4d	–	–	–	28 130[a]	11 080	3.15
$5p_{x,y}$	31 790	8490	3.60	–	–	–
$5p_z$	32 640	7640	3.79	31 650	7560	3.81
5d	33 730	6550	4.09	32 710	6500	4.11
5d	34 170[a]	6110	4.24	33 150	6060	4.26
$6p_{x,y}$	35 210[b]	5070	4.65	34 280	4930	4.72
$6p_z$	35 590[b]	4690	4.84	34 590	4620	4.87
6d	36 100[a]	4180	5.12	35 110	4100	5.17
6d	36 330[a]	3950	5.27	35 270[a]	3940	5.28
$7p_{x,y}$	36 820[b]	3460	5.63	35 820	3390	5.69
$7p_z$	37 090[b]	3190	5.87	36 090	3120	5.93

[a] Shoulder.
[b] Maxima of the peaks obtained from the Gaussian-fit analysis.

short-wavelength components of the R6p and R7p bands (Table 2) as the $p_{x,y}$ and p_z excitations, respectively. On going to $n = 5$ the splitting of Rydberg p transitions in **1** becomes obvious since the $R5p_{x,y}$ and $R5p_z$ peaks are observed separately in the absorption spectrum (Fig. 1). On the contrary, the spectrum of **2** shows in the $n = 5$ region only one Rydberg p peak at 31 650 cm^{-1}. The corresponding term value equals 7560 cm^{-1} which is very close to that of the $R5p_z$ transition in **1** (Table 2) as well as to the $T(R5p_z)$ value for $(\eta^6\text{-}1,3\text{-}C_6H_4Me_2)_2Cr$ (7620 cm^{-1} [4]). The term value for the $R5p_{x,y}$ excitations is noticeably higher (8490 and 8810 cm^{-1} for complex **1**(Table 2) and $(\eta^6\text{-}1,3\text{-}C_6H_4Me_2)_2Cr$ [4], respectively) so the peak at 31 650 cm^{-1} in the spectrum of **2** corresponds the $3d_{z^2} \rightarrow R5p_z$ excitation. The $R5p_{x,y}$ transition in **2** is predicted to lie at 30 700 cm^{-1} but there are no clearly defined absorption features in that part of the absorption spectrum. This Rydberg excitation is, therefore, broadened beyond detection because of configuration interactions. The interactions between Rydberg and intravalency excitations usually lead to the broadening of Rydberg peaks in the spectra of polyatomic molecules [8]. The Rydberg state of **2** resulting from the $3d_{z^2} \rightarrow R5p_{x,y}$ transition mixes, obviously, with the valence-shell excited states corresponding to band A (Fig. 1).

The first member of the Rnp_z series in both spectra is also broadened owing to an admixture of the intravalency excitations lying in the band A region. The $R4p_z$ transition is responsible for the shoulder at 25 400 cm^{-1} in the spectrum of **1** and at 25 110 cm^{-1} in the spectrum of **2**. The similar $R4p_z$ broadening was found

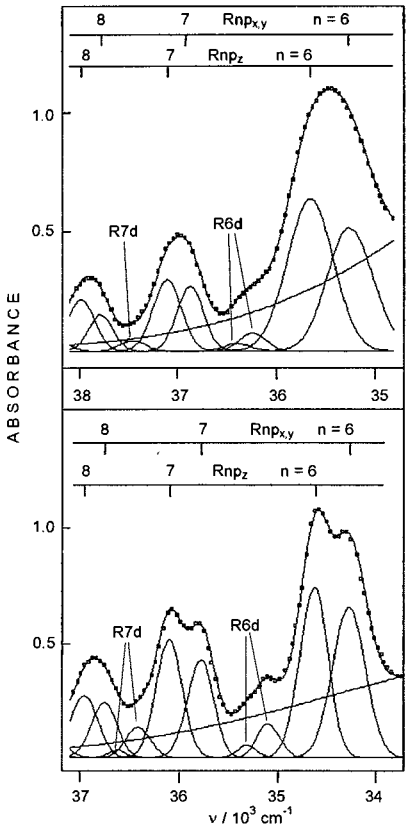

Fig. 2. Decomposition of Rydberg bands ($n = 6$–8) in the gas-phase spectrum of **1** (top) and **2** (bottom) into a sum of Gaussian peaks. The experimental curve is given by points.

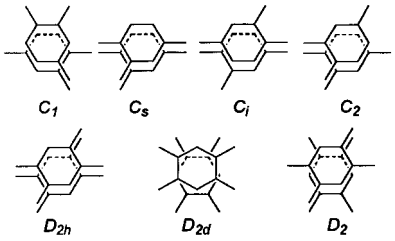

Fig. 3. Possible point groups for molecule **1** (top) and **2** (bottom).

for other chromium bisarene complexes [3,4]. It is difficult to determine unambiguously the valence-shell transitions mixing with the low-lying Rydberg excitations. According to the MS X_α MO calculations [11], peak A in the spectrum of $(\eta^6\text{-}C_6H_6)_2Cr$ arises from the metal-to-ligand charge transfer transition. It has been shown, however, that such assignment is not reliable [12].

The structures of the $R4p_{x,y}$ band for **1** and **2** are different. In the spectrum of **1** this band is split into two peaks of close intensities while the spectrum of **2** reveals one narrow $R4p_{x,y}$ peak (Fig. 1). This difference can well result from the molecular symmetries of **1** and **2**. Possible point groups are given in Fig. 3. There are two variants of ligand combination when forming molecule **1**. Mutual rotation of arenes gives four point groups (C_1, C_s, C_i and C_2). Molecule **2** can adopt the D_{2h}, D_{2d} or D_2 conformations. The irreducible representations corresponding to the Rydberg states and the optical selection rules [13,14] for one-photon transitions of the $3d_{z^2}$ electron to the Rydberg MOs are presented in Table 3. In all groups possible for **1** the $p_{x,y}$ levels are non-degenerated so transitions $3d_{z^2} \rightarrow Rnp_x$ and $3d_{z^2} \rightarrow Rnp_y$ can be observed as separate peaks. Naturally, the difference in energy for the Rnp_x and Rnp_y states decreases as n increases and for $n > 5$ one $p_{x,y}$ peak is seen in the spectrum of **1**.

Among possible conformations of **2** (Fig. 3), only D_{2d} gives degenerated $p_{x,y}$ orbitals (Table 3). The presence of one narrow absorption peak arising from the $R4p_{x,y}$ transition in the spectrum of **2** (Fig. 1) agrees with the D_{2d} molecular geometry of the gas-phase complex. This conclusion is confirmed by the analysis of other Rydberg transitions.

There are some Rydberg bands in the gas-phase spectra of **1** and **2** besides those belonging to the p series. The spectrum of **1** (Fig. 1) shows an intense long-wavelength peak at 22 300 cm^{-1} which must be interpreted as $3d_{z^2} \rightarrow R4s$ on the basis of its term value (Table 2). The presence of this band leads us to a conclusion that the C_i conformation, where the s excitations are forbidden (Table 3), is not preferable and free molecules of **1** adopt the C_1, C_s or C_2 geometry (Fig. 3). On going to the gas-phase spectrum of **2**, the R4s peak disappears (Fig. 1) which agrees with the selection rules (Table 3). Vibronically allowed components of the R4s transition contribute to a very weak shoulder at 22 200 cm^{-1} in this spectrum (Fig. 1).

In the region between the R4p and R5p excitations one should expect to find the $3d_{z^2} \rightarrow R4d$ transitions. However, they lie close to the intense valence excitations contributing to peak A so the corresponding bands can be broadened because of configuration interactions. The same situation takes place for other methylated derivatives of bis(η^6-benzene)chromium [4]. In the spectrum of **1** no Rydberg features can be revealed in the R4d region while the spectrum of **2** shows a shoulder at 28 130 cm^{-1} with the term value (Table 2) appropriate for its assignment as $3d_{z^2} \rightarrow R4d$.

On the other hand, the R5d excitations are seen as the well-resolved features for both complexes. In each case two R5d components can be revealed (Fig. 1 and Table 2). The higher Rydberg d excitations are also observed. There are weak shoulders at 36 100 and 36 330 cm^{-1} in the spectrum of **1** as well as a peak at 35 110 cm^{-1} and a shoulder at 35 270 cm^{-1} in the

Table 3
Irreducible representations[a] of the electronic states resulting from excitations of the $3d_{z^2}$ electron to the Rydberg s, p and d MOs in the point groups possible for **1** and **2**

MO	**1**				**2**		
	C_1	C_s	C_i	C_2	D_{2h}	D_{2d}	D_2
s	A(x, y, z)	A′(x, y)	A_{1g}(f)	A(x)	A_g(f)	A_1(f)	A(f)
p_x	A(x, y, z)	A′(x, y)	A_u(x, y, z)	A(x)	B_{3u}(x)	E(x, y)	B_3(x)
p_y	A(x, y, z)	A′(x, y)	A_u(x, y, z)	B(y, z)	B_{2u}(y)	E(x, y)	B_2(y)
p_z	A(x, y, z)	A″(z)	A_u(x, y, z)	B(y, z)	B_{1u}(z)	B_2(z)	B_1(z)
$d_{x^2-y^2}$	A(x, y, z)	A′(x, y)	A_{1g}(f)	A(x)	A_g(f)	B_1(f)	A(f)
d_{xy}	A(x, y, z)	A′(x, y)	A_{1g}(f)	B(y, z)	B_{1g}(f)	B_2(z)	B_1(z)
d_{xz}	A(x, y, z)	A″(z)	A_{1g}(f)	B(y, z)	B_{2g}(f)	E(x, y)	B_2(y)
d_{yz}	*A*(x, y, z)	A″(z)	A_{1g}(f)	A(x)	B_{3g}(f)	E(x, y)	B_3(x)
d_{z^2}	A(x, y, z)	A′(x, y)	A_{1g}(f)	A(x)	A_g(f)	A_1(f)	A(f)

[a] The polarisation of optically allowed transitions (x, y, z) is given in parentheses; forbidden excitations are indicated (f).

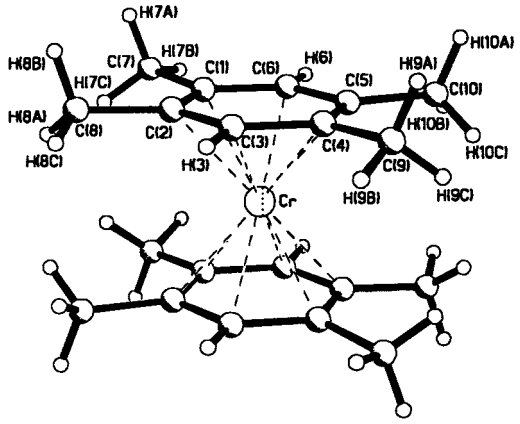

Fig. 4. The X-ray structure of **2**. The Cr–C distances in **2** (Å): Cr–C(1) 2.175(2), Cr–C(2) 2.175(2), Cr–C(3) 2.151(2), Cr–C(4) 2.175(2), Cr–C(5) 2.174(2), Cr–C(6) 2.149(2).

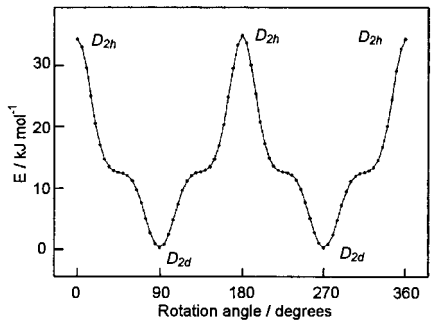

Fig. 5. The non-bonded repulsion energy E at various angles of mutual ligand rotation around the line, connecting the ring geometrical centres in **2,** calculated with use of the MOLDRAW package [14], the ligand geometry being fixed. The initial point corresponds to the eclipsed conformation (Fig. 4).

spectrum of **2** which correspond to the R6d transitions. The n^* values increase by ~ 1 on going from the R5d features to R6d (Table 2) as it is predicted by theory. The Gaussian-fit analysis reveals R7d components between R7p and R8p (Fig. 2). The observation of two Rydberg d components for $n = 5$, 6 (Fig. 2 and Table 2) is in good agreement with the prediction made on the basis of the selection rules for the D_{2d} point group (Table 3).

3.2. Molecular structure of (η^6-1,2,4,5-$C_6H_2Me_4$)$_2$Cr

The presence of intense Rnd bands in the spectrum of **2** demonstrates that the D_{2h} conformation (Fig. 3) cannot be preferable since in this point group Rnd transitions are optically forbidden. The appearance of one narrow R4p$_{x,y}$ peak and two Rydberg d components for $n = 5$, 6 agrees with the D_{2d} geometry best of all (Table 3).

On the contrary, the X-ray diffraction study of the crystal structure of **2** undertaken in this work gives the eclipsed conformation of the ligands in **2** (Fig. 4). In the crystal structure the Cr atom is in an inversion centre. The benzene ring in **2** is planar within ± 0.0003 Å. The deviations of the C(7), C(8), C(9),C(10) and Cr atoms from the average ring plane are -0.076, -0.076, -0.067, -0.061 and 1.637 Å, respectively. The Cr–C(ring) distances in **2** are in the narrow range 2.150–2.175 Å. The two shortest Cr–C(ring) distances corresponding to the non-substituted C atoms (Cr–C(3) 2.151(2) Å and Cr–C(6) 2.149(2) Å) are slightly longer than those found in bis(η^6-benzene)chromium (2.143, 2.140 Å [15]). Thus the symmetry of the molecule of **2** in crystal state is very close to D_{2h}.

The eclipsed position of methyl groups in the solid-state **2** is surprising since such ligand arrangement should correspond to a maximal non-bonded repulsion between two ligands. The repulsion energy at various angles of mutual ligand rotation around the line connecting the ring geometrical centres in **2** has been calculated in this work using the MOLDRAW package [16] on the basis of the molecular structure of **2**. This program computes the conformational energies based on the Buckingham model potentials [17]. The energy barriers obtained for **2** (Fig. 5) seem to be too high, being comparable with those derived experimentally (variable-temperature NMR) for the complex with bulky *tert*-butyl substituents (ca. 35 kJ mol^{-1} [18]). The qualitative trends are, however, quite reasonable. The plot (Fig. 5) has two maxima (0° and 180°) and two minima (90° and 270°). The lowest energy corresponds to the staggered conformations of the methyl groups as expected. The D_{2d} geometry should, therefore, be preferable for the free molecule of **2**. This agrees well with the analysis of the Rydberg structure in the gas-phase absorption spectrum of **2** given above. The D_{2h} conformation of **2** in the solid phase can well be a result of crystal packing effects providing a close packing of the molecules in the crystal structure of **2**. Methylated arene fragments such as 1,2,4,5-tetramethylbenzene in organometallic molecules can be efficiently 'locked in' by the surroundings [19].

3.3. Influence of ring methylation on the ionisation energies and Rydberg term values

The Rydberg parameters of **1** and **2** obtained in this work together with those found earlier for other bisarene complexes [3,4] make it possible to study the influence of ring methylation on the I and T values. Knowing IP of **2** we can check whether the linear dependence of the ionisation energy upon the number of methyl groups in the benzene rings of bis(η^6-arene)chromium [10] is maintained for the complex bearing eight substituents. For the derivatives bearing up to three CH_3 groups in each ring, the linear regression analysis based on the high-accurate ionisation

energies of bis(η^6-benzene)chromium [3] and its methylated derivatives (the previous research [4] and this work) gives the correlation equation as follows:

$$I(\text{eV}) = 5.449 - 0.076m;\ r = 0.99857,\ s = 0.010\ \text{eV}.$$

where $m = 0$–6 is the total number of methyl fragments in a bisarene molecule. Using this expression one can calculate IP of **2** to be 4.841 eV which is very close to that found from the Rydberg frequencies (Table 1). The decrease of IP caused by introduction of each subsequent CH_3 group into the ring is, therefore, equal up to $m = 8$ showing no mutual influence of substituents for the complexes considered.

Owing to observation of clearly defined bands arising from the R4s, R4p and R5p transitions in the spectra of **1** and **2** (Fig. 1) we can construct a correlation diagram for the term values of low-lying Rydberg excitations on the basis of the data obtained in this work and our earlier results [3,4]. The decrease in the T(R4s) magnitudes on methylation resembles that in the ionisation energies (Fig. 6). The $T(\text{R4p}_{x,y})$ values decrease also but to a less extent since Rydberg s MOs are more penetrative than p orbitals [8,20]. However, for $n = 5$ the picture is different. The $T(\text{R5p}_{x,y})$ and $T(\text{R5p}_z)$ parameters change in an irregular manner on introducing the CH_3 groups into the rings. They increase on going from benzene to toluene and xylene; then they decrease on further substitution (Fig. 6). Such a behaviour suggests that the influence of methylation on the Rydberg term values includes some mechanisms working in opposite ways.

On the one hand, appearance of methyl groups change the distribution of electron density because of the inductive effect. This results in an increased electron–electron repulsion and, correspondingly, in decreased IPs of the occupied valence-shell MOs which is revealed by the photoelectron spectroscopy [21]. Since the Rydberg term values represent the ionisation energies of Rydberg electrons one should expect that a similar trend will be observed for the T magnitudes. On the other hand, on appearance of methyl groups the size of the molecular core and the polarizability of the molecule grow resulting in the larger binding energies of Rydberg electrons. This mechanism leads, therefore, to an increase in the Rydberg term values. The total result is determined by the combination of the two mechanisms.

For the lowest Rydberg transitions, the average radii of Rydberg MOs in sandwich molecules are comparable with the molecular core size [12,22] so the dependence of the term values on the number of methyl groups should be similar to that of the ionisation energies corresponding to the non-bonding intravalency orbitals. The first mechanism dominates in this case. On going to $n = 5$ the sizes of Rydberg orbitals grow significantly [12,22] so the role of the second mechanism becomes more important. This can well result in the increased T(R5p) values for the complexes bearing two or four methyl substituents (Fig. 6). On going to **2**, however, a decrease in the R5p term values occurs since the large total inductive effect of eight CH_3 groups makes the electron–electron repulsion to be the main cause of the T(R5p) changes. It can be expected that for higher n the character of the term value dependence will resemble that for $n = 5$ but the influence of methylation should be weaker. Indeed, comparison of the term values of **1** and **2** (Table 2) with those of the bisarene complexes bearing benzene, toluene and xylene ligands [3,4] shows that the T(R6p) magnitudes depend on $m(CH_3)$ in a fashion similar to T(R5p) but the differences in the term values are smaller. Thus, the two mechanisms considered above explain well the observed trends in the influence of ring methylation on the Rydberg term values. An additional contribution to the shifts of the T magnitudes can arise from the configuration interactions changing on methylation.

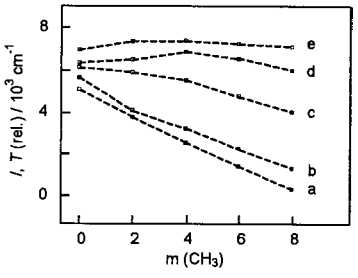

Fig. 6. Correlation diagram for the relative $3d_{z^2}$ ionisation energies I (a) and the term values of Rydberg transitions T(R4s) (b), $T(\text{R4p}_{x,y})$ (c), $T(\text{R5p}_{x,y})$ (d) and $T(\text{R5p}_z)$ (e) in the molecules of the bis(η^6-benzene)chromium derivatives bearing $m(CH_3)$ methyl groups. The I(rel.) and T(rel.) magnitudes were obtained by subtracting a constant number from the ionisation energy or term values for each $m(CH_3)$. The $T(\text{R5p}_{x,y})$ magnitude for $m(CH_3) = 8$ was taken as 7930 cm^{-1} which was calculated on the basis of the quantum defect $\delta = 1.18$ equal to that for $T(\text{R6p}_{x,y})$ in **2**.

4. Conclusions

Complexes **1** and **2** represent convenient objects for studying the influence of methyl substituents on the Rydberg structures in the absorption spectra of chromium bisarene derivatives. The gas-phase spectra of both compounds show narrow Rydberg bands arising from the transitions originating at the non-bonding chromium $3d_{z^2}$ orbital. These bands can be interpreted unambiguously on the basis of the corresponding term values and quantum defects. The convergence limit of the Rydberg p series gives the first ionisation potential as 4.994 ± 0.009 and 4.862 ± 0.009 eV for **1** and **2**, respectively.

New information on the electronic and molecular structures of bisarene complexes has been obtained in

this work. Changes of the relative Rydberg intensities observed on ring methylation result mainly from the different molecular symmetries and configuration interactions characterising sandwich complexes bearing methyl groups in the rings. The Rydberg spectra of **1** and **2** appear to reflect adequately the molecular geometries. The point group C_i for **1** and the group D_{2h} for **2** appear to be not dominant in the gas phase. The Rydberg structures agree with the C_1, C_s or C_2 conformation for **1** and the D_{2d} geometry for **2** in the gas phase. The preferability of the D_{2d} geometry for the free molecule of **2** is confirmed by calculation of energies of the non-bonded repulsion between the ligands. In crystal, however, this molecule adopts an eclipsed conformation close to D_{2h}.

The data obtained in this work make it possible to analyse systematically for the first time the influence of methyl groups on the term values of Rydberg excitations in sandwich molecules. The first ionisation potential of bisarene complexes decreases in a linear fashion as the number of methyl groups in the rings increases from zero to eight. The term values of the lowest Rydberg s and p transitions diminish monotonely on methylation while the T(R5p) magnitudes grow on going from the benzene to the xylene complexes and then decrease on further ring methylation. The difference in the trends for the term values corresponding to $n = 4$ and 5 can well be explained by combination of the methyl group inductive effect with a growth of the molecular core size and increase in the core polarizability on methylation.

Acknowledgements

This research was partly financed by the Russian Foundation for Basic Research (Grants N 00-03-32853, 00-15-97439, 00-03-32807). S.K. is grateful to the Royal Society of Chemistry for the financial support within the Journals Grants to the International Authors program and to the Foundation for Fatherland Science Assistance. The authors thank Dr Yu.B. Makarov for working out a computer program for Gaussian-fit analysis of the gas-phase absorption spectra.

References

[1] G.A. Domrachev, S. Yu. Ketkov, G.A. Razuvaev, J. Organomet. Chem. 328 (1987) 341.
[2] S.Yu. Ketkov, G.A. Domrachev, G.A. Razuvaev, J. Mol. Struct. 195 (1989) 175.
[3] S.Yu. Ketkov, J.C. Green, C.P. Mehnert, J. Chem. Soc. Faraday Trans. 93 (1997) 2461.
[4] S.Yu. Ketkov, G.A. Domrachev, C.P. Mehnert, J.C. Green, Russ. Chem. Bull. 47 (1998) 868.
[5] S.Yu. Ketkov, in: F. Kajzar, V.M. Agranovich (Eds.), Multiphoton and Multielectron Driven Processes in Organics: New Phenomena, Materials and Applications, Kluwer, Dordrecht, 2000, p. 503.
[6] P.L. Timms, J. Chem. Soc. Chem. Commun. (1969) 1033.
[7] F.G.N. Cloke, M.L.H. Green, J. Chem. Soc. Dalton Trans. (1981) 1938.
[8] M.B. Robin, Higher Excited States of Polyatomic Molecules, vol. 1, Academic Press, New York, 1974.
[9] Bruker, SHELXTL, Version 5.10, Bruker AXS Inc., Madison, WI, USA, 1998.
[10] J.C. Green, Struct. Bonding (Berlin) 43 (1981) 37.
[11] J. Weber, M. Geoffroy, A. Goursot, E. Penigault, J. Am. Chem. Soc. 100 (1978) 3995.
[12] S.Yu. Ketkov, C. Mehnert, J.C. Green, Chem. Phys. 203 (1996) 245.
[13] G. Herzberg, Molecular Spectra and Molecular Structure, III. Electronic Spectra of Polyatomic Molecules, Van Nostrand, New York, 1966.
[14] R.L. Flurry Jr., Symmetry Groups. Theory and Chemical Applications, Prentice-Hall, Englewood Cliffs, 1980.
[15] E. Keulen, F. Jellinek, J. Organometal. Chem. 5 (1966) 490.
[16] P. Ugliengo, G. Borzani, D. Viterbo, J. Appl. Crystallogr. 21 (1988) 75.
[17] M.A. Spackman, J. Chem. Phys. 85 (1986) 6579.
[18] U. Zenneck, Ch. Elschenbroich, R. Moeckel, J. Organomet. Chem. 219 (1981) 177.
[19] D. Braga, Chem. Rev. 92 (1992) 633.
[20] M.B. Robin, Higher Excited States of Polyatomic Molecules, vol. 3, Academic Press, Orlando, 1985.
[21] S. Evans, J.C. Green, S.E. Jackson, B. Higginson, J. Chem. Soc. Dalton Trans. (1974) 304.
[22] S.Yu. Ketkov, J. Organometal. Chem. 465 (1994) 225.